Manipulation of the electrosprayed dielectric fluids using electric fields

Robert L. Garris, Maciej A. Noras
Dept. of Engineering Technology
University of North Carolina at Charlotte
phone: (1) 704-687-5053
e-mail: mnoras@uncc.edu

***Abstract*— the objective of this work was to demonstrate control of electrosprayed dielectric liquid using electric fields. The main focus of the investigation was on maximizing the charging of the fluid, charging repeatability, and on control of the position of electrosprayed droplets within a confined volume. Triboelectric charging was a method of choice, as the liquid used in tests (gasoline) is flammable. The charge to mass ratio was measured using a Faraday pail for different spray injection pressures and various injection times. The charge applied to the liquid was in the range of -0.1 to -0.4 nC/g. The location and the shape of the electrosprayed plume of droplets was then manipulated using electric fields. The experimental results were used in validation of the FEA simulations of the process.**

I. INTRODUCTION

Electrospraying is a century old technique [1] that has been vastly utilized in many fields of science and technology. One of the unique applications for which it has also been considered is atomization and dispersion of fuel in the injection process in car engines [2]. When the fuel droplets are small and well mixed with air, the combustion process afterwards is cleaner and more complete [3, 4]. In gasoline and diesel engines, depending on a type of injector features, the droplet Sauter mean diameter (SMD, defined as the diameter of the droplet with the same surface to volume ratio as that of the overall spray) is in the range of 120–200 μm [5]. Electrospraying allows that number to change to much finer ranges, values as low as 10 μm have been reported [6, 7]. The process works well in atmospheric pressures [8]. Achieving appropriate atomization and fuel to air ratio is just an initial step into the injection process. Typical pressures in a cylinder of a car reach up to 20 MPa (Diesel engines) and that prevents the fuel from dispersing properly within the engine's cylinder. In order to entrain the fuel further into the cylinder volume, very high injection pressures have to be used. First implementation of electrospraying in a working car engine was demonstrated by Anderson [9], but the gains in engine performance and reduction in emissions were relatively small. The electrosprayed droplets were not penetrating the cylinder depth sufficiently, and had tendency to drift toward the grounded walls. The resulting recommendations were to increase the fuel charging and introduce appropriate control techniques. No specific methods were proposed, however in the earlier work by Shrimpton [2] a suggestion was made to attempt controlling the plume of electrosprayed fuel by use of electric AC or DC fields, however no practical implementation of that idea was provided. This paper presents an attempt on control of electrosprayed fuel using external electric fields in an engine cylinder-like geometry. The focus of the work was on

providing better entrainment of the charged plume into the cylinder volume.

II. Forces acting on charged droplets

This topic has been studied extensively by many researchers (for example, [10, 11]). As the charged fuel jet leaves the spray injection nozzle, it encounters several kinds of forces acting upon droplets

A. Mechanical

- aerodynamic force (drag),

Drag force on a single spherical droplet moving with a vector velocity u [10]:

$$F_{drag} = 6\pi\eta D_p u \qquad (1)$$

Dp – droplet diameter,
η – air kinetic viscosity,
u is the particle velocity vector in the air (air is considered as still, nonmoving medium).

Since the pressures in the engine's cylinder are high, it is necessary to consider non-continuum effects associated with droplet collisions under highly pressurized air. A mean free path λ in the air is:

$$\lambda = \frac{\mu}{0.499 \cdot p\sqrt{\frac{8M}{\pi RT}}} \qquad (2)$$

In the equation above, μ is air viscosity 1.8 10^{-5} [kg/(m*s)], p is pressure [Pa], M is molecular weight 0.02896 [kg/mol], T is temperature [K], R is molar gas constant 8.3145 [J/(mol K)]. A typical mean free path for a pressure of 6 MPa at the temperature of 298 K is λ=1.1 nm. If the droplet radius exceeds 1.1 nm then the gas appears to it as a continuum. In case of larger droplets, the non-continuum effects need not to be considered

- gravitational force on a single spherical droplet

$$F_{\text{gravity}} = gm_p \qquad (3)$$

where g is the gravity constant 9.81 [m/s^2], mp is the particle mass, which can be computed using fuel density and a particle diameter.

B. Electrical

- Forces due to electric fields created in the volume

$$F_{\text{el}} = qE \qquad (4)$$

C. Total force acting upon a particle

$$m_p \frac{du}{dt} = \sum F = 6\pi\eta D_p u + gm_p + qE \qquad (5)$$

III. Controlling droplet movement

The goal is to direct the sprayed plume of charged particles into the depth of the engine's cylinder, suppressing movement of the droplets toward walls of the cylinder. The drag force and electric field force need to be directed against the force that makes droplets move

toward the wall of the cylinder. Let's consider horizontal components only (subscript x added), which eliminates gravity force:

$$m_x \frac{du_x}{dt} = -6\pi\eta D_p u_x - qE_x \qquad (6)$$

Let's assign a variable $\tau = 6\pi\eta D_p$.

The solution is then

$$u_x = \frac{-qE_x}{\tau}\left(1 - e^{\frac{-t}{t_m}}\right) + u_{x0}e^{\frac{-t}{t_m}} \qquad (7)$$

Where $t_m = m_p/\tau$ t_m is the mechanical relaxation time. This tells how the droplet will respond to external electrical force: if the force is applied for the time that is short as compared to the relaxation time, the behavior of the droplet will be ruled by its inertia. Otherwise it will be controlled by drag forces.

The distance which particle travels horizontally is

$$x = \frac{-qE_x}{\tau}\left[t - t_m\left(1 - e^{\frac{-t}{t_m}}\right)\right] + u_{x0}t_m\left(1 - e^{\frac{-t}{t_m}}\right) + x_0 \qquad (8)$$

Assuming that the fuel droplets are charged to maximum value predicted by Rayleigh limit:

$$q = 8\pi\sqrt{\varepsilon_0\eta\left(\frac{D_p}{2}\right)^3} \quad (9)$$

η is the surface tension of gasoline, (a typical example value used here was 0.0258 N/m, derived for 87 octane gasoline at 20 [°C]), ε_0 is dielectric permittivity of air $8.85 \cdot 10^{-12}$ [F/m], D_p is particle diameter. The equation predicts the maximum charge that the droplet can handle before it breaks up into smaller droplets. For example, the maximum charge for gasoline droplet with 10 µm diameter is 0.13 pC.

An example calculation of the distance traveled toward wall was carried out for typical values of: $m_p=3.92\times10^{-13}$ [kg], $D_p=10\cdot10^{-6}$ [m], $\eta=43.7\times10^{-6}$ [Pa·s], $q=100\times10^{-15}$ [C]. Assuming x0=0 [m], initial position of the particle and u_{x0}=80 [m/s], initial x direction velocity of the particle, it can be observed (Figure 1) that the drag force is dominating the droplet behavior.

After 0.4 ms, due to inertia, the presence of the electrical force becomes apparent and the droplet starts moving away from the wall. This computation is done for laminar motion of the particles and, in addition, does not take into account space charge force from the presence of other charged droplets.

IV. Modeling

Concept of controlling the sprayed fuel cone was modeled using Comsol Multiphysics software. A model was constructed to simulate the results of high pressure injections of electro-sprayed fuel into a pressurized cylinder with and without an electric field applied. These models (Test 1 and Test 2) were used to demonstrate the dynamic movement of the fluid created by the electric fields inside of the chamber. The spray chamber geometry consisted of a two section cylinder with a diameter of 10 cm (3.937 in) and a total height of 20 cm (7.37 in) in ambient air conditions. Two separate sections were used to mimic

the engine's cylinder and create the electric field distribution needed to direct the fuel droplets.

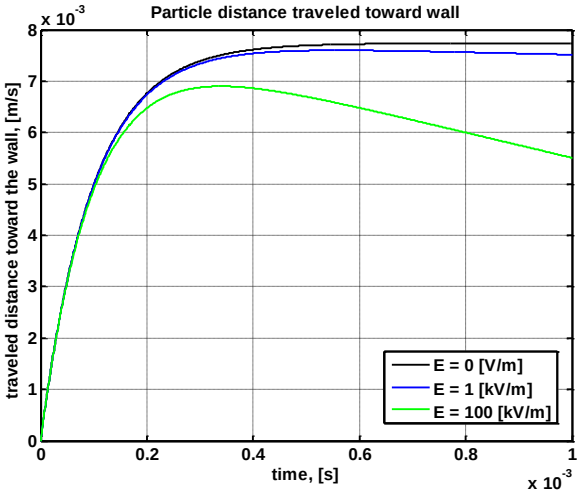

Figure 1: Particle distance traveled toward wall for different electric field intensities

A. Case 1, no electric field applied.

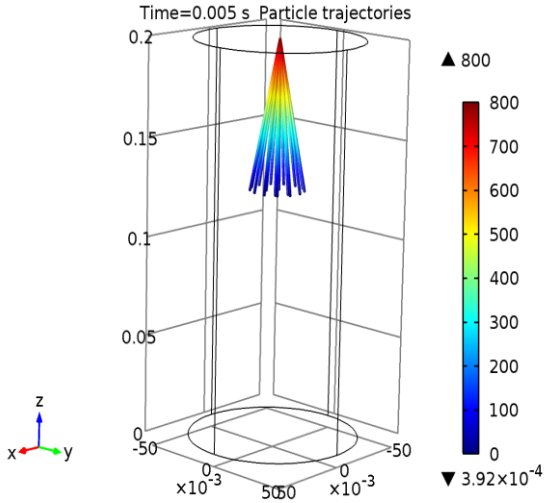

Figure 2: Droplet trajectories without the electric field

Error! Reference source not found. shows the spray particle trajectories. Penetration after 5ms reaches approximately 0.75 meters from the release point at z = 0.2 m. A total of 20 spherical droplets are injected at a cone angle of 30°. The droplets sizes are assumed to remain constant. The droplets came into a halt after 5 ms due to drag forces.

B. Electric field applied to upper part of the cylinder

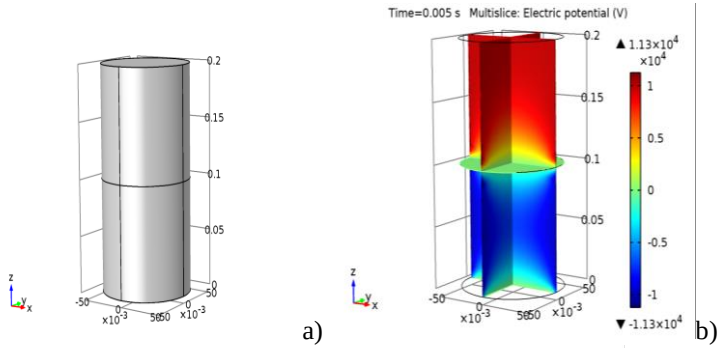

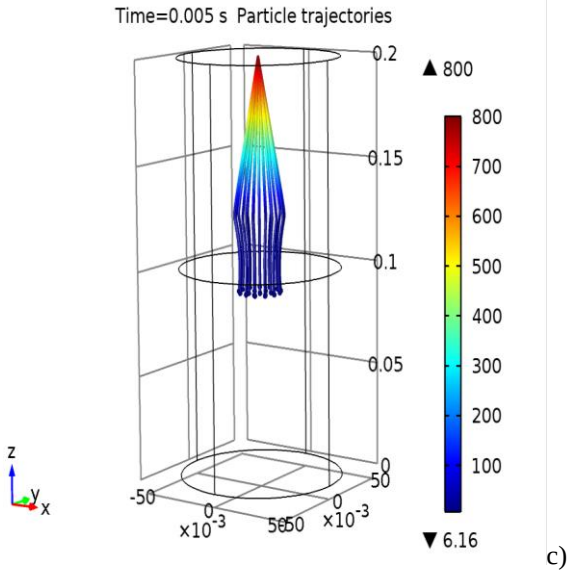

Figure 3: Electric field applied. a) cylinder geometry, b) electric potential applied, c) droplet trajectories.

In this case the droplets are charged as previously, but the positive potential is applied to the upper part of the cylinder. This results in suppression of the droplet movement toward the walls, as shown in Figure 3 and the negative potential applied to the bottom part of the cylinder drags the droplets toward the bottom. Penetration is much deeper, at approx. 0.12 m. The potentials applied are +10 kV and – 10 kV.

V. Experiment

A. Design of the test fixture

To further this investigation, a test spray chamber and injection unit was designed and tested. This unit was used to investigate the theory discussed above to control charged fuel droplets. 87 Octane gasoline was collected from a local gas station and

tested for charging magnitude and repeatability of charge. Triboelectric charging was implemented as the source for inducing the charge in the fuel. A section of the piping was changed between teflon and nylon.

Controlling the direction movement of the injected fuel was attempted by creating an electric field to repel and attract the fuel droplets. The field was created by applying a negative potential to the top metal section of the spray chamber. The droplets are charged negatively; therefore they should be repelled from the walls toward the center. The bottom section of the chamber was grounded, thus attracting the sprayed fuel. Initial estimation for operating injection pressure was in the range from 10 to 30 PSI. The pressure was generated by a diaphragm pump, and was monitored by a pressure gage located in the flow path of the fuel. Initially a push valve was implemented to restrict the flow and to release the injection processes. After the initial test, an automated valve was implemented to increase the consistence of injection time of each spray. It was controlled using an SEL 2411 programmable logic controller. The block diagrams for the test set up is shown in Figure 4 and Solidworks rendering in Figure 5.

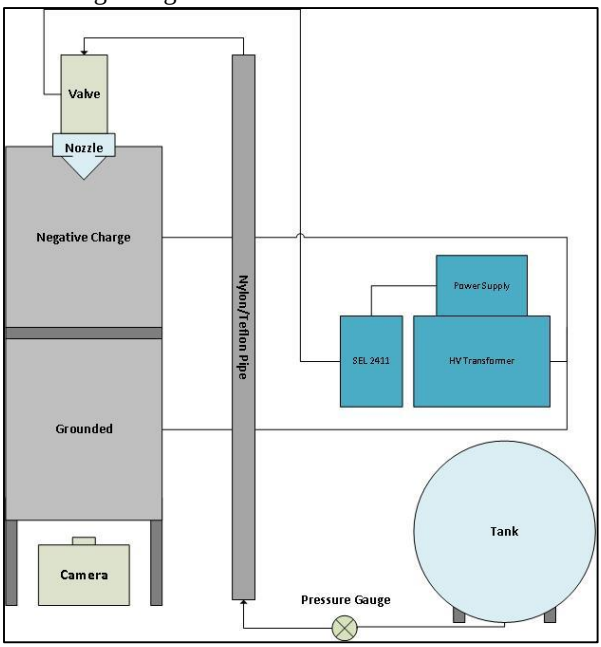

Figure 4: Test chamber layout.

To generate the electric field, a high voltage source, capable of applying 10 kV was used. To capture the injection a high speed camera was placed at in front of the injection chamber and a mirror was set at an angle to reflect the event. A high intensity light source was used to aid the camera's ability to capture the event. The details of the setup are presented in Figure 6.

Figure 5. Solidworks rendering of the test chamber.

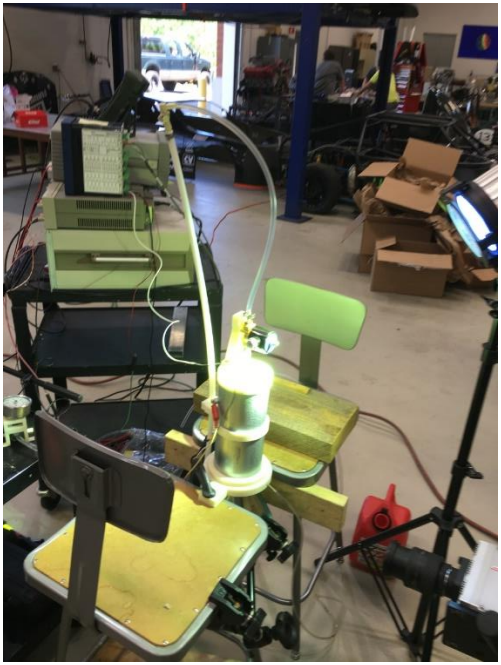

Figure 6. Display of the test setup.

The high voltage amplifier (Trek 10/10B) to supply10 kV to the upper section of the chamber while the lower section of the chamber was grounded. Both section were made

of 4" diameter thin walled steel piping. This resulted in an application of an electric charge to the fuel as soon as it exited the injector and entered the cylinder.
The high speed camera (Red Lake Motion-Xtra HG-XR) views the event that is conducted in the chamber at 1000 frames per second, the image is reflected via mirror placed at an angle under the glass bottom of the cylinder.

Motion Studio software, which is supported by Innovation in Motion (IDT) was used to compare all the recordings. Individual frames were evaluated over the range of injection times. The injection profile was evaluated over the transition period from the nozzle to the middle section of the chamber. During the recorded amount of frames in which the event took place, eight measurements were taken for each of the four experiments. Measurement distance from the nozzle can be seen in Figure 7 below.

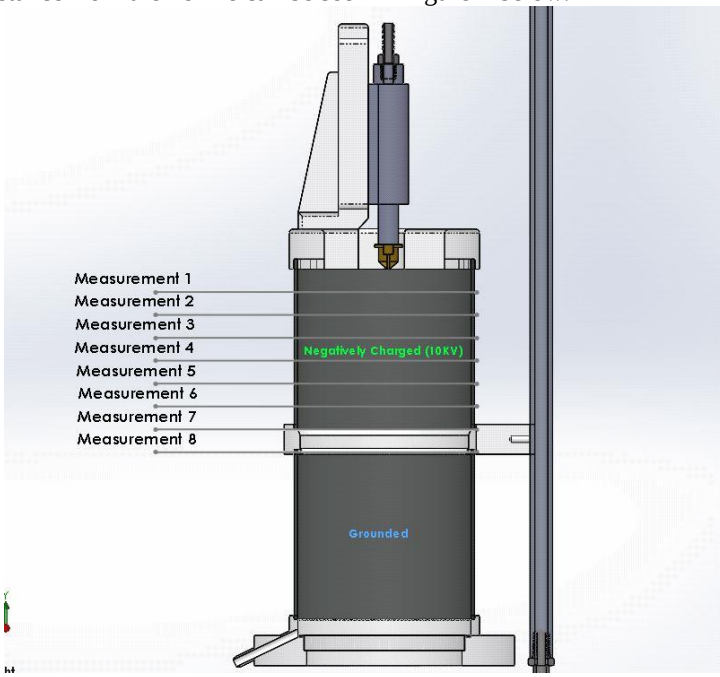

Figure 7: Measurement locations from the nozzle in the injection chamber.

B. Test results

The initial results for charge repeatability and magnitude showed that the charge applied to the liquid was in the range of -0.1 to -0.4 nC/g and that 88.75% of the values for all injection pressures were found to be within +/- 0.05 nC/g from the mean. Original equipment included a push button valve where the time of injection was dependent on the operator's ability to maintain a constant spray time. The tubing section for the specified materials was lengthened to increase overall net charge. By increasing the pipe length by one foot, the net charged increased. However, the magnitude increase of the overall net charge was not significant. Theoretically, if the pipe continued to be lengthened the injection charge would increase. An automated valve was installed to maintain a consistent

spray time and it was observed that 100% of the values fell within +/- 0.05 nC/g. However, due to more uniform injection times the deviation of the charge magnitudes decreased to -0.1 to -0.3 nC/g. The maximum charge was recorded at 20 PSI using teflon piping. Refer to Table 1 below for all charging results. All the tests were carried out using Keitthley 6517B electrometer and a Faraday pail.

Table 1. Fuel charging results.

Injection Pressure [PSI]	Charging Material [Teflon - 2"]	Charge [μC]	Standard Deviation	Charge Density [nC/g]	Charging Material [Nylon -	Charge [μC]	Standard Deviation	Charge Density [nC/g]
15	Teflon	-0.00267	0.00009	-0.252	Nylon	-0.00238	0.00008	-0.224
15	Teflon	-0.00265		-0.250	Nylon	-0.00245		-0.231
15	Teflon	-0.00262		-0.247	Nylon	-0.00235		-0.221
15	Teflon	-0.00271		-0.255	Nylon	-0.00254		-0.239
15	Teflon	-0.00260		-0.245	Nylon	-0.00250		-0.236
15	Teflon	-0.00266		-0.251	Nylon	-0.00250		-0.236
15	Teflon	-0.00261		-0.246	Nylon	-0.00262		-0.247
15	Teflon	-0.00261		-0.246	Nylon	-0.00254		-0.239
15	Teflon	-0.00276		-0.260	Nylon	-0.00262		-0.247
15	Teflon	-0.00239		-0.225	Nylon	-0.00253		-0.238
Averages		-0.00263		-0.248		-0.00250		-0.236
Injection Pressure [PSI]	Charging Material [Teflon - 2"]	Charge [μC]	Standard Deviation	Charge Density [nC/g]	Charging Material [Nylon -	Charge [μC]	Standard Deviation	Charge Density [nC/g]
20	Teflon	-0.00324	0.00009	-0.264	Nylon	-0.00272	0.00012	-0.222
20	Teflon	-0.00325		-0.265	Nylon	-0.00285		-0.232
20	Teflon	-0.00324		-0.264	Nylon	-0.00278		-0.227
20	Teflon	-0.00315		-0.257	Nylon	-0.00255		-0.208
20	Teflon	-0.00326		-0.266	Nylon	-0.00276		-0.225
20	Teflon	-0.00301		-0.245	Nylon	-0.00269		-0.219
20	Teflon	-0.00322		-0.263	Nylon	-0.00284		-0.232
20	Teflon	-0.00320		-0.261	Nylon	-0.00258		-0.210
20	Teflon	-0.00319		-0.260	Nylon	-0.00287		-0.234
20	Teflon	-0.00300		-0.245	Nylon	-0.00294		-0.240
Averages		-0.00318		-0.259		-0.00276		-0.225
Injection Pressure [PSI]	Charging Material [Teflon - 2"]	Charge [μC]	Standard Deviation	Charge Density [nC/g]	Charging Material [Nylon -	Charge [μC]	Standard Deviation	Charge Density [nC/g]
25	Teflon	-0.00304	0.00014	-0.222	Nylon	-0.00282	0.00018	-0.206
25	Teflon	-0.00297		-0.217	Nylon	-0.00266		-0.195
25	Teflon	-0.00290		-0.212	Nylon	-0.00279		-0.204
25	Teflon	-0.00302		-0.221	Nylon	-0.00240		-0.176
25	Teflon	-0.00305		-0.223	Nylon	-0.00242		-0.177
25	Teflon	-0.00275		-0.201	Nylon	-0.00248		-0.181
25	Teflon	-0.00302		-0.221	Nylon	-0.00233		-0.171
25	Teflon	-0.00277		-0.203	Nylon	-0.00235		-0.172
25	Teflon	-0.00314		-0.230	Nylon	-0.00234		-0.171
25	Teflon	-0.00322		-0.236	Nylon	-0.00270		-0.198
Averages		-0.00299		-0.219		-0.00253		-0.185
Injection Pressure [PSI]	Charging Material [Teflon - 2"]	Charge [μC]	Standard Deviation	Charge Density [nC/g]	Charging Material [Nylon -	Charge [μC]	Standard Deviation	Charge Density [nC/g]
30	Teflon	-0.00270	0.00024	-0.186	Nylon	-0.00294	0.00030	-0.203
30	Teflon	-0.00248		-0.171	Nylon	-0.00249		-0.172
30	Teflon	-0.00264		-0.182	Nylon	-0.00260		-0.180
30	Teflon	-0.00201		-0.139	Nylon	-0.00208		-0.144
30	Teflon	-0.00220		-0.152	Nylon	-0.00200		-0.138
30	Teflon	-0.00204		-0.141	Nylon	-0.00224		-0.155
30	Teflon	-0.00241		-0.166	Nylon	-0.00240		-0.166
30	Teflon	-0.00225		-0.155	Nylon	-0.00278		-0.192
30	Teflon	-0.00210		-0.145	Nylon	-0.00212		-0.146
30	Teflon	-0.00260		-0.180	Nylon	-0.00219		-0.151
Averages		-0.00234		-0.162		-0.00238		-0.165

With 20 PSI and teflon as the charging material four injections were tested and results were evaluated. Based on visual observation, some initial effects were determined. They indicated that the fuel droplets, when injected into a 10 kV electric field, were affected by compressing the fuel profile. These initial results were verified by measuring the four injection profiles at the eight locations seen in Figure 7. In Motion Studio, calibration of the viewing area was conducted using the diameter (110.3mm) of the cylinder as shown in Figure 8

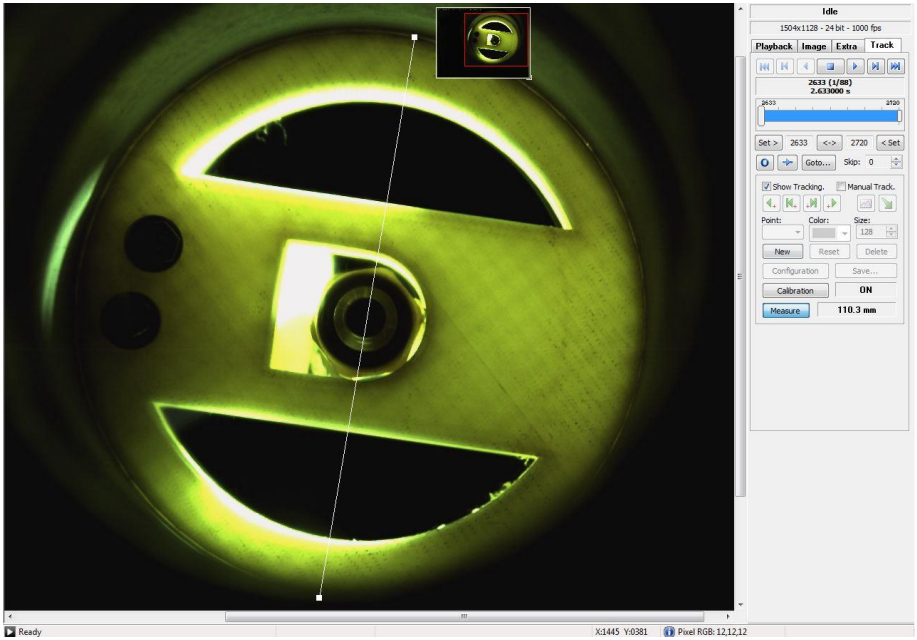

Figure 8. Processing high speed camera pictures using In Motion Studio software.

Measurement of the fuel profile was determined for both the X and Y directions for all four injections. For each experiment, the injection pressure was 20 PSI and at a room temperature of 75°F. All X and Y measurements for the four different injections are represented in Table 2 - 5.

Table 2: Measurements of Injection 1 (No Electric Field)

Injection Pressure (+/- 2 PSI)	Temperature (°F)	Measurement Depth From Nozzle (mm)	X Measurement (mm)	Y Measurement (mm)
20	75	14.5	5.7	7.7
20	75	29.0	6.9	8.8
20	75	43.6	6.8	10.6
20	75	58.1	7.0	11.7
20	75	72.6	8.8	13.5
20	75	87.1	11.6	15.5
20	75	101.6	15.3	23.8
20	75	116.2	25.4	27.9

Table 3: Measurements of Injection 2 (Electric Field Applied)

Injection Pressure (+/- 2 PSI)	Temperature (°F)	Measurement Depth From Nozzle (mm)	X Measurement (mm)	Y Measurement (mm)
20	75	14.5	5.1	5.1
20	75	29.0	4.4	6.5
20	75	43.6	3.9	7.3
20	75	58.1	3.7	8.6
20	75	72.6	5.9	10.2
20	75	87.1	10.6	12.7
20	75	101.6	14.4	17.0
20	75	116.2	21.1	20.4

Table 4: Measurements of Injection 3 (No Electric Field)

Injection Pressure (+/- 2 PSI)	Temperature (°F)	Measurement Depth From Nozzle (mm)	X Measurement (mm)	Y Measurement (mm)
20	75	14.5	7.7	8.6
20	75	29.0	7.9	10.1
20	75	43.6	5.9	11.1
20	75	58.1	5.5	12.6
20	75	72.6	6.4	13.8
20	75	87.1	11.7	14.4
20	75	101.6	17.7	20.3
20	75	116.2	24.7	26.8

Table 5: Measurements of Injection 4 (Electric Field Applied)

Injection Pressure (+/- 2 PSI)	Temperature (°F)	Measurement Depth From Nozzle (mm)	X Measurement (mm)	Y Measurement (mm)
20	75	14.5	5.5	6.5
20	75	29.0	6.1	6.1
20	75	43.6	6.1	7.0
20	75	58.1	5.4	8.6
20	75	72.6	4.6	10.4
20	75	87.1	10.9	12.6
20	75	101.6	18.0	18.6
20	75	116.2	24.6	26.5

Solid Works was used to generate the fuel profiles based on the measurements of the X and Y direction of each injection. An example comparison is shown in Figure 9. Each injection profile was reconstructed by sketch planes at the eight distances from the nozzle. Injection models were then mated in the assembly to compare the width of the profiles and to give a visual of the compression of the fuel cloud with the electric field applied.

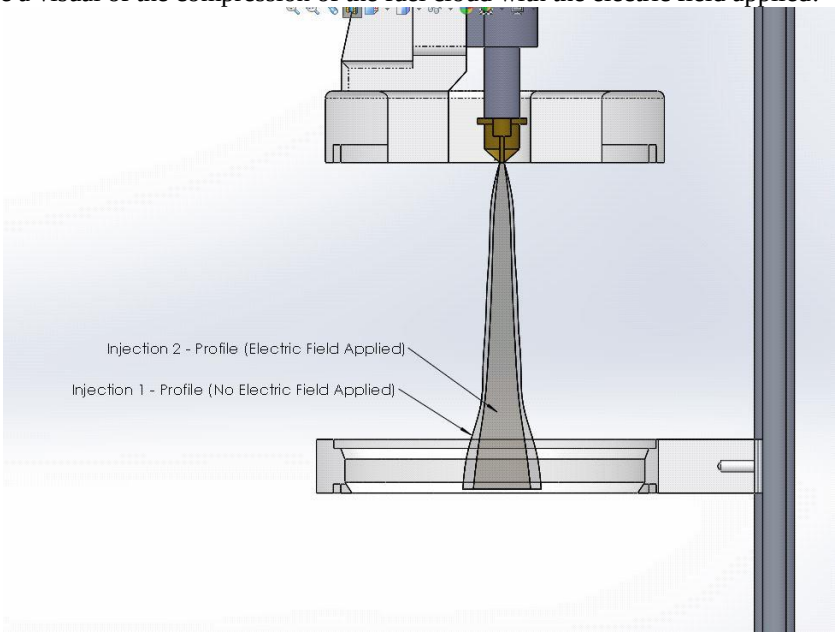

Figure 9: Example generated profile comparison of Experiments 1 & 2.

VI. Conclusion

Experimental results for the repeatability showed that the fuel was able to acquire and hold a net charge during injection using both teflon and nylon piping. Teflon showed better charging results over the different injection pressures.

High speed camera imaging had shown that over four different injections the fuel profile created was uniform with and without the electric field applied for both specific test cases. When comparing all injections it can also be seen that the electric field forces compress the fuel cloud in the X and Y direction achieving control over the fuel profile. Further research will be done to investigate the optimization of liquid control using electric fields for IC engines.

References

[1] J. Zeleny, "The Electrical Discharge from Liquid Points, and a Hydrostatic Method of Measuring the Electric Intensity at Their Surfaces," *Physical Review*, vol. 3, pp. 69-91, 02/01/ 1914.

[2] J. S. Shrimpton, "Pulsed charged sprays: application to DISI engines during early injection," *International Journal for Numerical Methods in Engineering*, vol. 58, pp. 513-536, 2003.

[3] E. L. Keating, *Applied combustion*. Boca Raton: CRC Press/Taylor & Francis, 2007.

[4] S. McAllister, J.-Y. Chen, and A. C. Fernandez-Pello, "Droplet Evaporation and Combustion," in *Fundamentals of Combustion Processes*, ed New York, NY: Springer New York, 2011, pp. 155-175.

[5] G. Fiengo, A. di Gaeta, A. Palladino, and V. Giglio, "Basic Concepts on GDI Systems," in *Common Rail System for GDI Engines: Modelling, Identification, and Control*, ed London: Springer London, 2013, pp. 17-33.

[6] U. Leuteritz, A. Velji, and E. Bach, "A novel injection system for combustion engines based on electrostatic fuel atomization," in *International Spring Fuels and Lubricants Meeting and Exposition, June 19, 2000 - June 22, 2000*, Paris, France, 2000.

[7] L. Li, S. Yu, and Z. Hu, "Theoretical and experimental studies of electrospray for IC engine," in *2006 SAE World Congress, April 3, 2006 - April 6, 2006*, Detroit, MI, United states, 2006.

[8] E. K. Anderson, D. C. Kyritsis, A. P. Carlucci, and A. De Risi, "Electrostatic effects on gasoline direct injection in atmospheric ambiance," *Atomization and Sprays*, vol. 17, pp. 289-313, 2007.

[9] E. Anderson, D. Kyritsis, R. Coverdill, and C.-F. Lee, "Experimental Evaluation of Electrostatically Assisted Injection and Combustion of Ethanol-Gasoline Mixtures for Automotive Applications," 2010.

[10] R. C. Flagan and J. H. Seinfeld, *Fundamentals of air pollution engineering*. Englewood Cliffs, N.J.: Prentice Hall, 1988.